Rock Mech. Rock Engng. (2003) 36 (2), 163–179
DOI 10.1007/s00603-002-0041-1

Rock Mechanics and Rock Engineering
Printed in Austria

Technical Note

An Evaluation of Image Analysis Algorithms for Constructing Discontinuity Trace Maps

By

J. Hadjigeorgiou[1], **F. Lemy**[1], **P. Côté**[1], and **X. Maldague**[2]

[1] Department of Mining, Metallurgy and Materials Engineering, Université Laval, Quebec City, Canada
[2] Department of Electrical Engineering, Université Laval, Quebec City, Canada

Received January 19, 2001; accepted September 5, 2002;
Published online January 21, 2003

Keywords: Image analysis, discontinuity trace detection.

1. Introduction

Scanline mapping provides the means to characterize the rock mass surrounding an exposed excavation. This information is subsequently used to identify zones of similar geomechanical conditions and as input for analysis and design of excavations in rock. A major constraint is the difficulty in collecting good quality data as mapping can often be hindered by limited access, dust, poor lighting, noise as well as production constraints. Consequently, this has resulted in several mining operations exploring variations of traditional mapping with the aim to optimize data collection (Hadjigeorgiou et al., 1995). Unfortunately, experience has shown that gains in efficiency and speed of mapping can result in insufficient quality of the data.

In recent years, there has been a move towards employing shotcrete as a primary support. This often necessitates its prompt application, thus limiting the time available for mapping. Given such production constraints it is hence imperative to develop a quick and reliable methodology for recording structural data. This necessity has been the motivation for the present work to compare the performance of a series of algorithms in recognizing geological small-scale features from photographs.

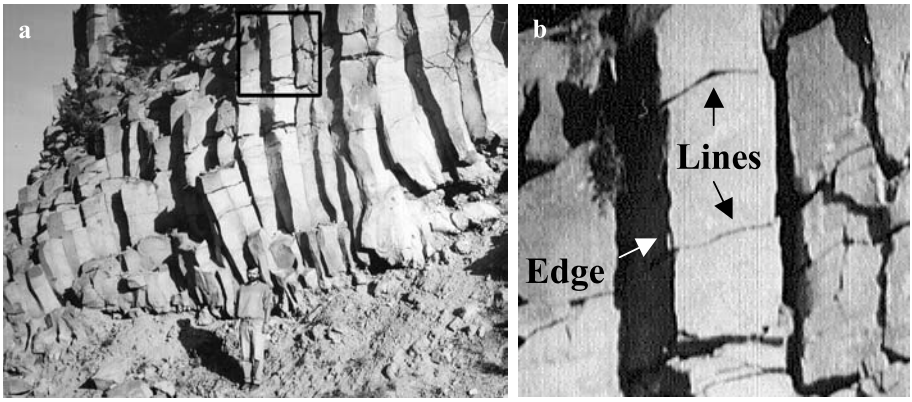

Fig. 1. **a** A well defined blocky rock mass; **b** A close up of the image identifying the distinction between lines and edges

2. Definitions

For the purposes of this paper, the following definitions are used with reference to digital images of discontinuities in rock:

a. Edge: A boundary between two regions of an image that have relatively distinct grey levels. Fig. 1 shows how an edge defines a joint.
b. Line: Curvilinear structure in an image that defines a joint in the rock mass, Fig. 1.
c. Topographic feature: A grey scale image is considered as a topographic map with dark pixels corresponding to low elevation and light pixels to high elevation. An example of a topographic feature is the 3D representation of an incision in Fig. 2b, which represents the joint shown in Fig. 2a.

A detection algorithm is used to delineate all pertinent geological features from digital images of discontinuities in rock. This is accomplished by assigning a relative intensity value to each pixel in the image. Thresholding is then used to establish the range of interest for the foreground in the resulting binary image. Figure 3a is an example where the relative intensity of each pixel in the image, is represented by a numerical value. If a threshold value of 5 is used then all pixels having a relative intensity greater than 5 are identified, as shown in Fig. 3b. The threshold is used as a filter, whereby only those pixels that meet the threshold are retained. This results in the transformation of the image to that represented in Fig. 3c.

A successful algorithm identifies all pixels that constitute a discontinuity trace at their proper location in the image. The performance of the investigated algorithms was evaluated based on the following criteria described in Fig. 4:

a. Detection criterion: A succesful algorithm has a high probability of extracting true features (pixels) and a low probability of extracting false features. Referring to Fig. 4a, the dark pixels represent the features to be detected. In Fig. 4b, it is noted that only some of the pixels of Fig. 4a are recognised. Furthermore,

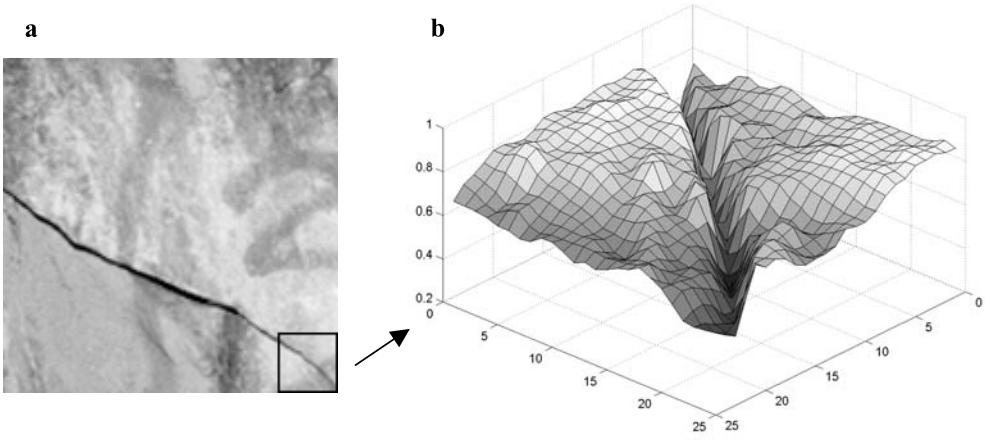

Fig. 2. **a** Discontinuity trace grey level image and **b** its corresponding light intensity function

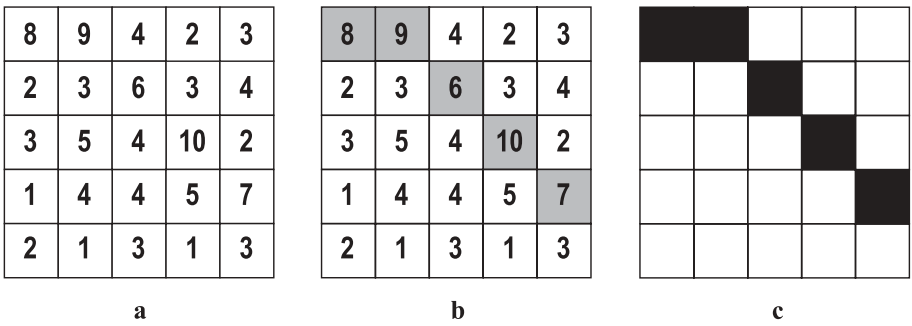

Fig. 3. An example application of a threshold

in certain cases, pixels are recognised even when no discontinuity trace is present. This detection criterion is implemented by quantifying recognition and error rates, further defined as:

i) $$\text{Recognition Rate} = \frac{\sum(\text{detected pixels corresponding to a feature})}{\sum(\text{pixels representing the feature})} \times 100\%$$

ii) $$\text{Error Rate} = \frac{\sum(\text{detected pixels not corresponding to a feature})}{\sum(\text{pixels in the image})} \times 100\%$$

Applying these definitions to Fig. 4b results in a recognition rate of 71.4% and an error rate of 7.8%.

b. Localization criterion: The extracted points should be as close as possible to the true points of a feature. Ideally, the localization of a detected trace should correspond to its actual location in the image. In Fig. 4c, all pixel features from Fig. 4a are in fact recognised. However, their localization in space is not nec-

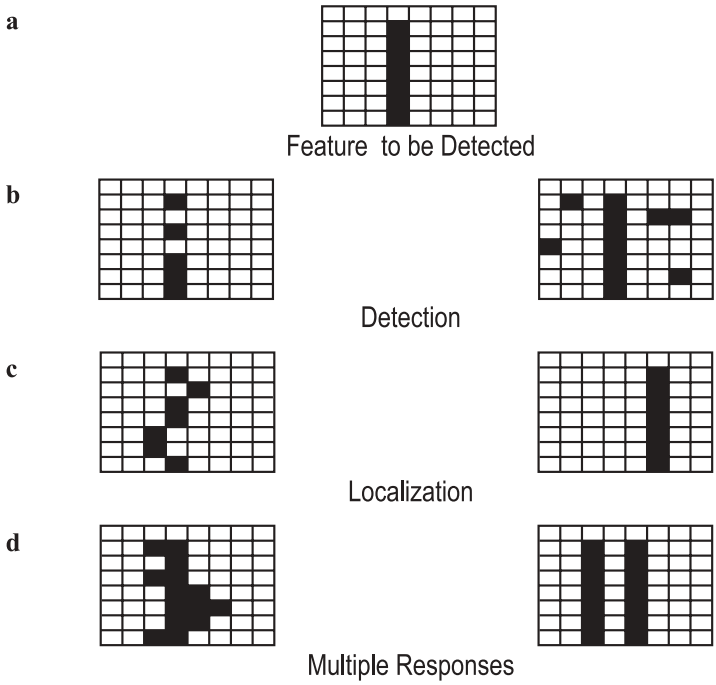

Fig. 4. Definition of feature detection criteria used to evaluate the performance of edge and line recognition algorithms

essarily correct. For example, in the diagram on the right, all pixels are translated to the right of the actual trace localization.

c. Multiple response criterion: In a successful application of a digital image analysis, it is necessary to ensure that the detection operator produces a unique result for a given feature. In Fig. 4d, the detection process results in multiple responses. Referring to Fig. 4a, the object to be detected is composed of 7 pixels. The detected features shown in Fig. 4d consist of 14 pixels.

For the purposes of this paper, in identifying discontinuities in rock, any localization errors and multiple responses were interpreted as failure of the detection algorithm.

3. Discontinuity Characterisation Using Image Analysis

In the past, stereoscopic methods have been employed to characterize geological structures from visual detection of discontinuity traces (Allam, 1978; Hagan, 1980; Rorke and Brummer, 1985; Harrison, 1993; Beer et al., 1999). An advantage of stereoscopic methods is that it is possible to determine joint orientation. Cheung et al. (1996) developed an imaging system based on a scanner that projects a light stripe illuminating the rock face and a pair of video cameras that captures the

image. This has allowed one to compute the 3D geometry of a rock exposure. Nevertheless, at the present time it would appear that the stereoscopic approach has several drawbacks including time-consuming fieldwork and data interpretation that requires expensive and somewhat cumbersome equipment. Recently Feng et al. (1999) developed a mapping system, using a Total Station, that determines the co-ordinates of selected points in the rock mass.

Tsoutrelis et al. (1990) and Crosta (1997) report on identifying and manually tracing discontinuities from photographic images. Manual tracing, however, is time consuming and has limited potential for practical applications. Maerz (1990), Reid and Harrison (2000) have developed methods to construct discontinuity trace maps by employing algorithms that consider an image as a continuous two dimensional light intensity function $f(x, y)$. In this case, x and y represent spatial co-ordinates at a point in the image plane. The value of the function at any point represents the brightness or gray level of the image at that point. The gray level image of a discontinuity trace, and its corresponding light intensity function, can be described by a three-dimensional surface as shown in Fig. 2. In this example, the discontinuity trace is easily recognizable by a deep and steep valley.

Maerz (1990) used a line detector developed by Dony (1988) to extract lines from an image using the first derivative of the filtered image in conjunction with a zero crossing detector. The elevation minima or maxima of the light intensity function correspond to changes in the sign of the first derivative of the image. The detected curves were then linked based on a series of simple geometrical conditions (distance and orientations). Reid and Harrison (2000) proposed a semi-automatic method for line reconstruction whereby an operator selects a seed pixel at one of the extremities of every perceived discontinuity. Once this is established, it is possible to reconstruct each discontinuity by joining all segments, constructed by pixels forming incisions in the image.

The works of Maerz (1990), Reid and Harrison (2000) demonstrate the great potential of digital face mapping. It would appear, however, that the employed algorithms were only tested for a limited range of rock conditions.

Furthermore, representing discontinuity traces as dark visible lines is not satisfactory for all types of ground conditions. This is illustrated in the photo of the blocky rock mass, Fig. 1. Using the definitions for edge and line adopted in this paper and referring to Fig. 1b it can be seen that rock blocks are defined by both edges and lines. A methodology that can accommodate both line and edge recognition, can then be applied to the majority of cases analysing the geological structures observed in a rock mass. These requirements define the basis of current work described below.

4. Evaluation of Edge and Line Detection Algorithms for Recognition of Discontinuity Traces

The authors conducted a critical review of image analysis literature and identified six detection algorithms for their potential for edge or line detection: Sobel described by Gonzalez and Wintz (1987); Johnson (1990); Canny (1986); Dony

Table 1. Algorithms evaluated for the detection of discontinuity traces

Detection algorithm	Detected object	Basic principle
Sobel	Edge	Thresholding of the first derivative of the light intensity function calculated at each pixel.
Johnson	Edge	Thresholding of the first derivative of the light intensity function calculated at each pixel. Local light intensity is accounted for.
Canny	Edge	Thresholding of the first derivative of the light intensity function calculated at each pixel.
Topographic	Line	Identification of pixels representing incisions in the light intensity function by calculating the maximum and minimum curvatures at each pixel.
Dony	Line	Identification of zero crossings of the light intensity function's first derivative calculated at each pixel. This is represented by a sign change between neighbouring pixels.
Steger	Line	Identification of zero crossings of the light intensity function's first derivative. This is calculated at each pixel in the direction where the second derivative is maximum.

(1988); Steger (1998) and a topographic operator reported by Wang and Pavlidis (1993), Lee and Kim (1995) as well as Reid and Harrison (2000). The selected algorithms along with a short description of their basic principles are summarized in Table 1.

The Sobel and Canny algorithms are probably the most popular edge detection algorithms. Both rely on filters to compute the image's first derivative. The Johnson algorithm is a modification of the Sobel detection algorithm that can account for varying conditions of scene illumination. The efforts of Dony (1988) and Reid and Harrison (2000) were of particular interest given their application to extracting discontinuity traces from rock exposures. Steger's implementation (1998), in the same way as Dony's algorithm, extracts lines using the first and second derivatives of a filtered image. Once applied to an image of a rock exposure, the algorithms result in a binary image with the black pixels corresponding to the detected features, and the white pixels to the others.

Université Laval has an extensive database of scanline and photographic data from several mines in the Canadian Shield. A series of photographic images were selected representing diverse field conditions. It should be noted that the photographs were taken during mapping, using a 35 mm camera and a flashlight as a source of illumination. At the time the photographs were taken, no effort was made to consider ideal lighting for image analysis. A main objective of this work is to develop procedures that can eventually be applicable for a range of geological and structural conditions.

The performance of the selected algorithms was evaluated with reference to the six images in Fig. 5. All images are of a standard size of 150×150 pixels corresponding to a rock face area of 30×30 cm.

In order to compare the performance of the selected algorithms, the detection, localization and multiple response criteria, summarized in Fig. 4, were used. As a

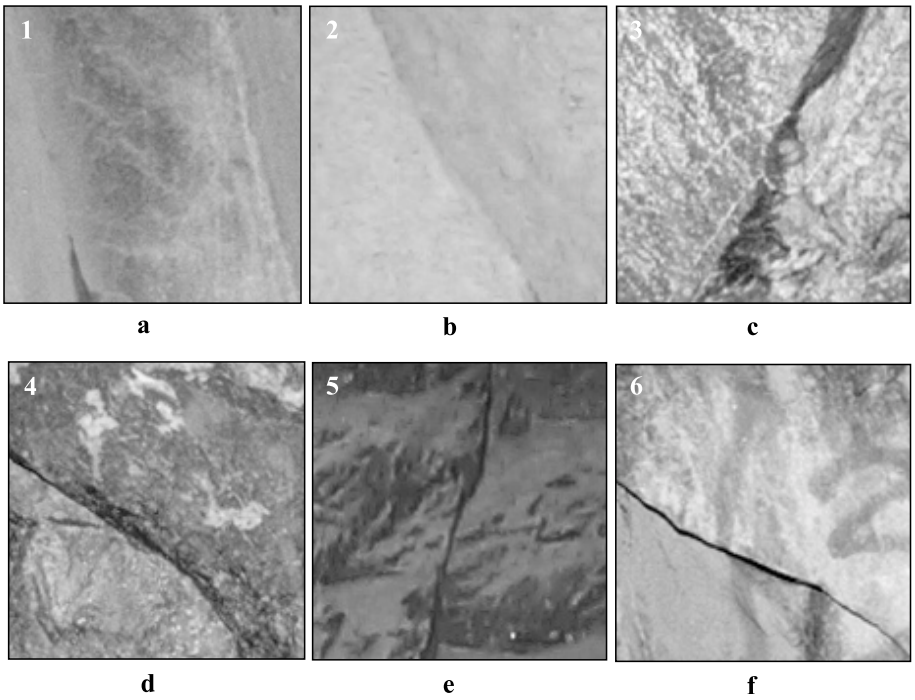

Fig. 5. Selected 30 × 30 cm photographic images of discontinuity traces: **a** Image 1 of a trace edge in a volcanic 'cap' rock; **b** Image 2 of a trace edge in rhyolite; **c** Image 3 of a trace edge in basalt; **d** Image 4 of a trace edge or line in basalt; **e** Image 5 of a trace line in rhyolite; **f** Image 6 of a trace line in a volcanic tuff

first check, the occurrence or absence of localization errors and/or multiple responses was investigated. A quantitative assessment of the detection criterion was undertaken by calculating error and recognition rates. For each image, a threshold specific to each detection algorithm was adjusted in order to obtain a maximum recognition rate while minimizing the error rate. The results are summarized in Table 2 and in Figs. 6 to 11.

5. Analysis of Results

Referring to Table 2, the Sobel, Johnson and Canny algorithms revealed no localization error or multiple response, for edge detection. An exception was when edges with low contrast had to be extracted. The presence of irregular edges in the images proved problematic for the Sobel and Johnson algorithms. Moreover, when lines represent discontinuity traces, edge detectors produced both localization errors and double responses corresponding to the two sides of the lines. This is shown in Fig. 11c illustrating Sobel edge detector applied to image 6. Given that the Dony and Steger algorithms are designed as line detectors it was not surprising

Table 2. Relative performance of the detection algorithms for the investigated images

Images	1	2	3	4	5	6
			Sobel			
R.R. max (%)	96.8	98.6	99.3	98.2	98.6	98.0
E.R. (%)	23.4	21.1	15.9	8.8	7.2	0.1
L.E.	yes	yes	no	no	yes	yes
M.R.	yes	yes	no	yes	yes	yes
			Johnson			
R.R. max (%)	96.2	98.6	96.6	97.6	95.3	92.6
E.R. (%)	21.9	20.2	4.3	3.1	1.7	0.1
L.E.	yes	yes	no	no	yes	yes
M.R.	yes	yes	no	yes	yes	yes
			Canny			
R.R. max (%)	94.2	98.6	99.3	98.2	98.0	98.7
E.R. (%)	16.2	17.6	4.1	4.0	14.9	0.0
L.E.	yes	yes	no	no	yes	yes
M.R.	yes	yes	no	no	yes	yes
			Topographic			
R.R. max (%)	58.0	95.9	96.6	94.1	95.9	93.3
E.R. (%)	6.1	5.8	10.0	7.2	6.3	1.7
L.E.	yes	yes	yes	yes	yes	yes
M.R.	yes	yes	yes	yes	yes	yes
			Dony			
R.R. max (%)	94.8	95.9	97.9	97.0	96.6	98.7
E.R. (%)	20.2	17.3	20.2	18.1	7.2	2.0
L.E.	yes	yes	yes	yes	yes	no
M.R.	yes	yes	yes	yes	no	no
			Steger			
R.R. max (%)	84.3	93.9	89.0	92.9	98.6	98.0
E.R. (%)	15.4	11.1	14.4	6.5	8.9	0.1
L.E.	yes	yes	yes	yes	no	no
M.R.	no	yes	yes	yes	no	no

R.R. max = Maximum Recognition Rate; E.R. = Error Rate;
L.E. = Location Error; M.R. = Multiple Response

that they had difficulties to detect edges. With respect to line detection, Steger creates well-localised lines while use of the Dony algorithm results in a localization error of one pixel. The employed topographic algorithm systematically generates both localization errors and multiple responses.

Referring to Figs. 6–11, the joints were manually traced and shown in Figs. 6b, 7b, etc. Recognition rates were evaluated by counting the number of pixels found in a neighborhood of 2 pixels around the manually traced joints. When the structural features are best described as edges such as in Figs. 6, 7 and 8, the maximum recognition rates for the Sobel, Johnson and Canny edge detectors were close to 100%. When lines best describe the joints, as in Figs. 10 and 11, very high recognition rates were attained. Referring to Table 2, the Topographic and Johnson operators were less successful with recognition rates of 93.3% and 92.6%.

It should be noted that one of the reasons for certain high recognition rates

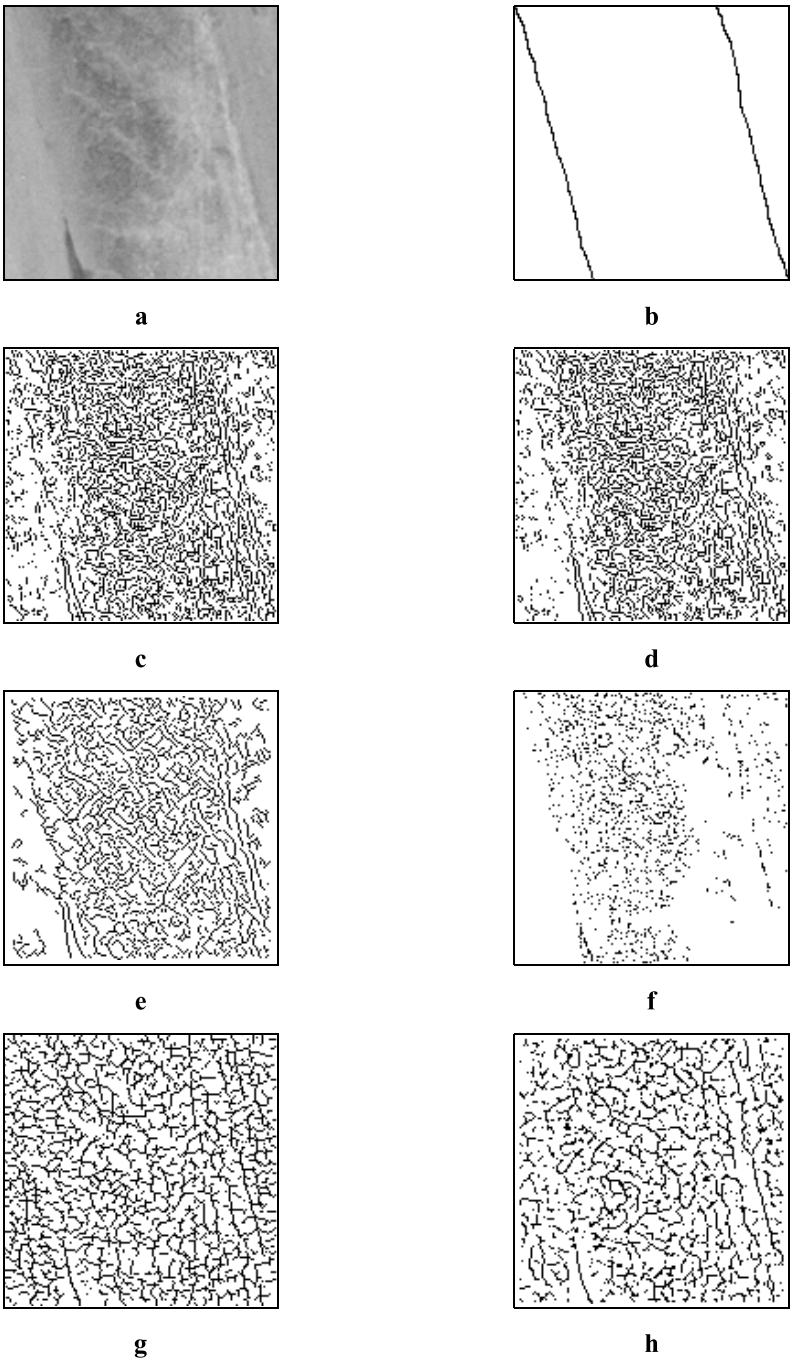

Fig. 6. **a** Photo image 1 representing a trace edge in a volcanic 'cap' rock; **b** Pertinent structural feature; **c** Sobel; **d** Johnson; **e** Canny; **f** Ravine pixel detection; **g** Dony; **h** Steger

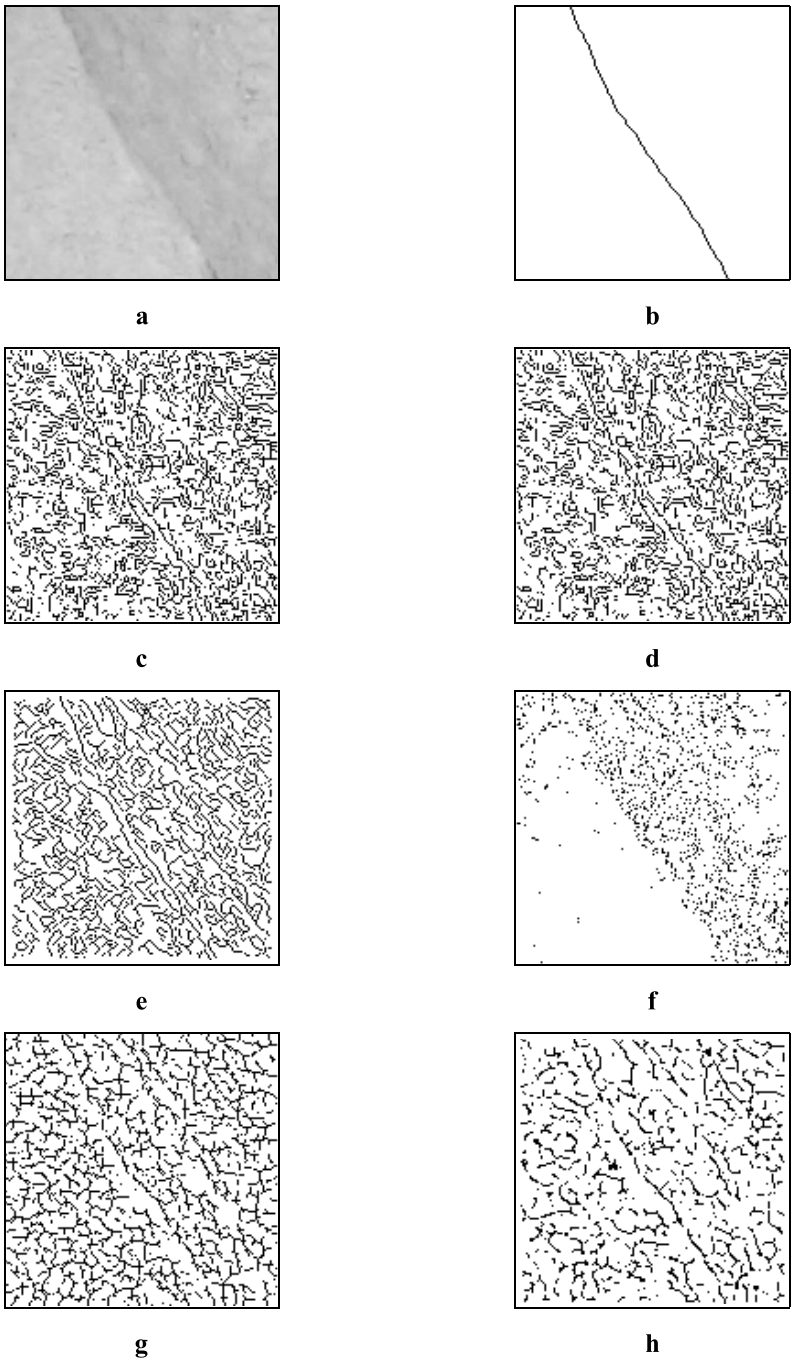

Fig. 7. **a** Photo image 2 representing a trace edge in rhyolite; **b** Pertinent structural feature; **c** Sobel; **d** Johnson; **e** Canny; **f** Ravine pixel detection; **g** Dony; **h** Steger

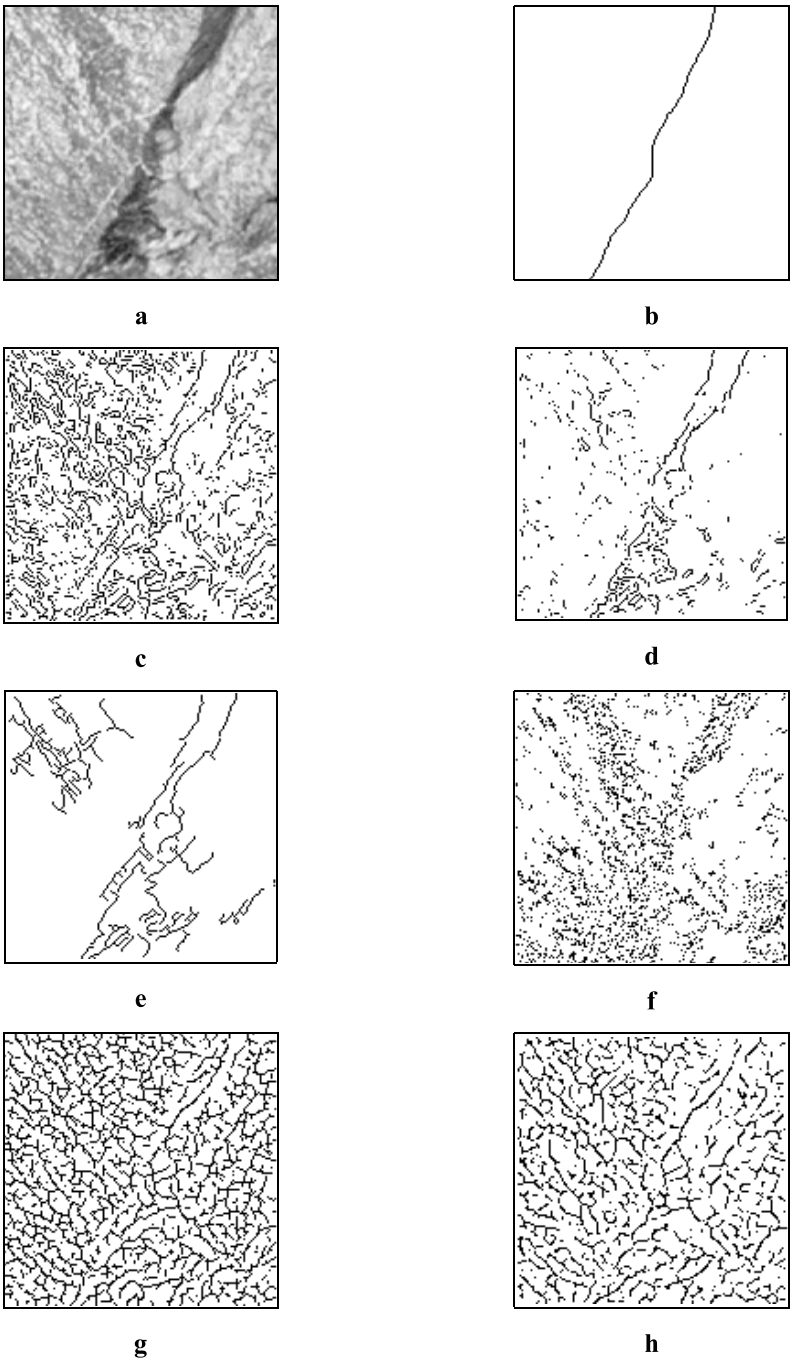

Fig. 8. **a** Photo image 3 representing a trace edge in basalt; **b** Pertinent structural feature; **c** Sobel; **d** Johnson; **e** Canny; **f** Ravine pixel detection; **g** Dony; **h** Steger

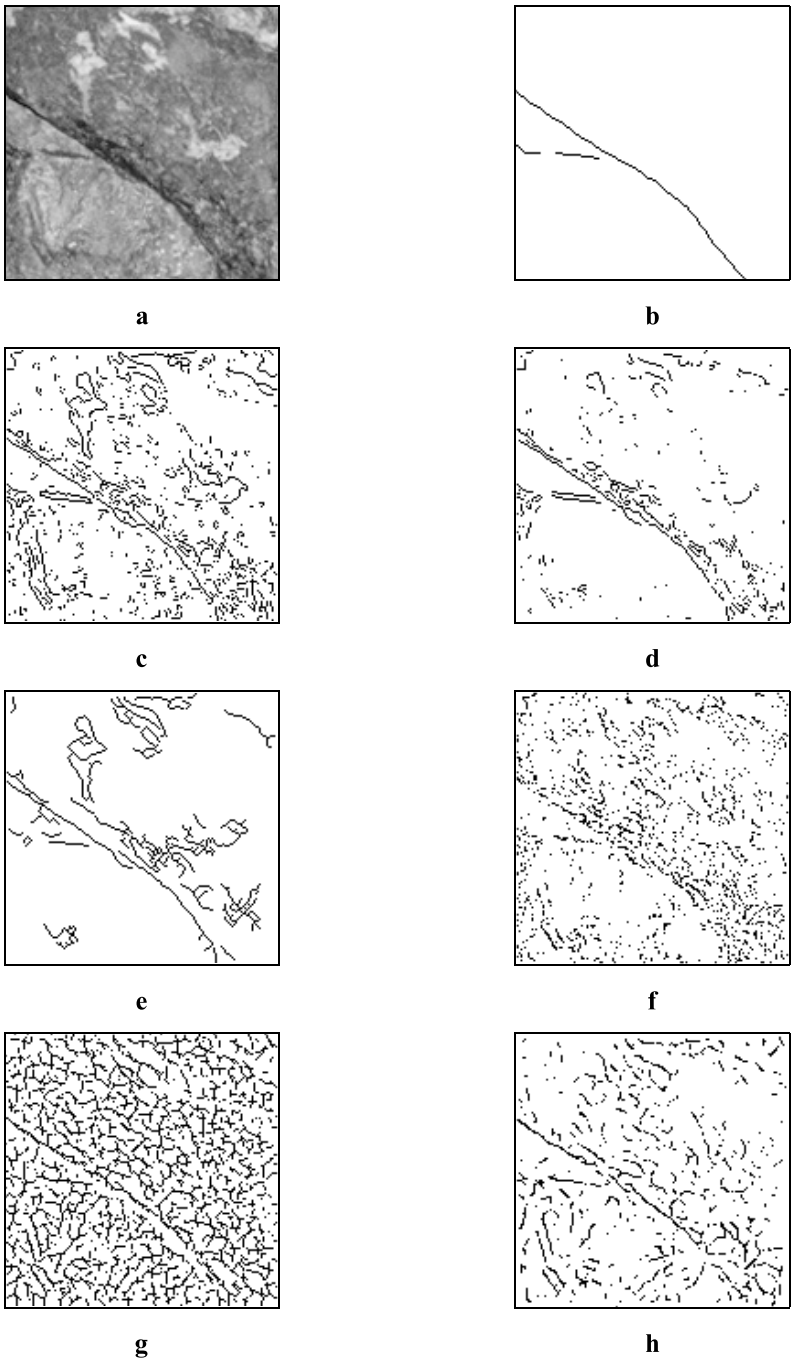

Fig. 9. **a** Photo image 4 representing a trace edge or line in basalt; **b** Pertinent structural feature; **c** Sobel; **d** Johnson; **e** Canny; **f** Ravine pixel detection; **g** Dony; **h** Steger

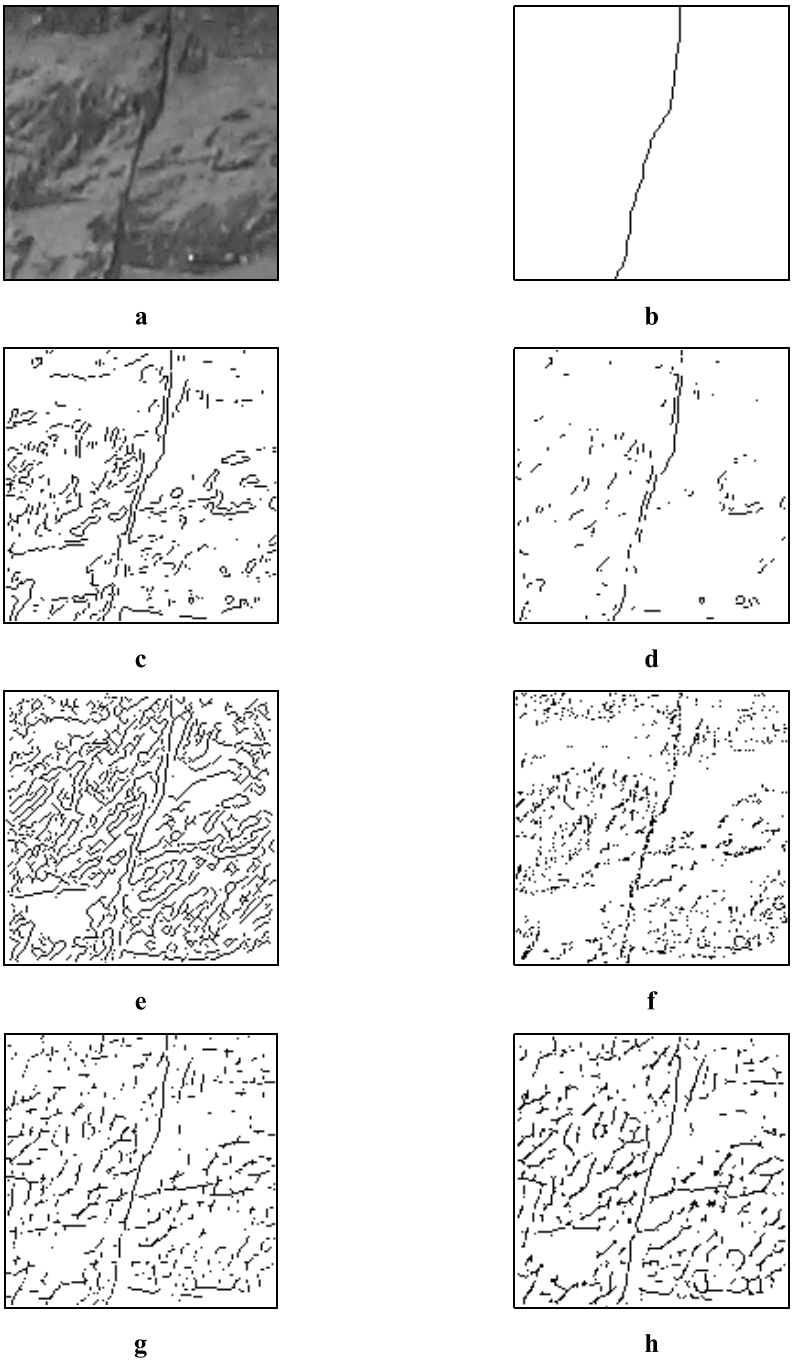

Fig. 10. **a** Photo image 5 representing a trace line in rhyolite; **b** Pertinent structural feature; **c** Sobel; **d** Johnson; **e** Canny; **f** Ravine pixel detection; **g** Dony; **h** Steger

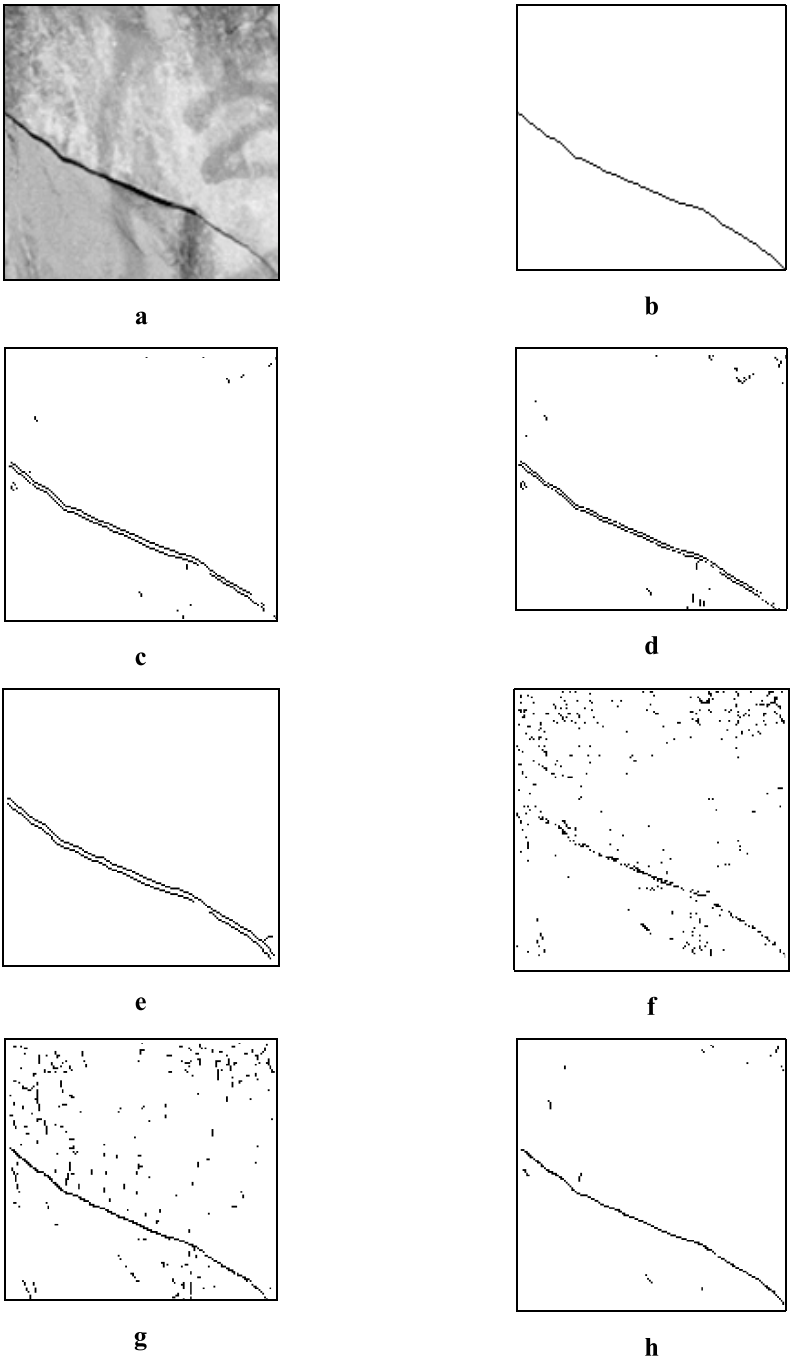

Fig. 11. **a** Photo image 6 representing a trace line in a volcanic tuff; **b** Pertinent structural feature; **c** Sobel; **d** Johnson; **e** Canny; **f** Ravine pixel detection; **g** Dony; **h** Steger

was a consequence of multiple responses. Consequently, recognition rates overestimate the actual performance of the topographic algorithm, as shown in Fig. 11f and in Table 2. A further drawback of the topographic method is the number of operations necessary to transform the high number of detected incision pixels, into segments and eventually discontinuity traces.

Where detected pixels do not correspond to geological features of interest, this results in high error rates (Table 2). Error rates are greatly influenced by image contrast and rock texture. Where joint traces are delineated by edges, the Johnson and Canny operators produce less erroneous responses than the Sobel algorithm. It was not clear, at the time of the work, which line detection algorithm minimizes the error rate when lines represent joints.

6. Conclusions

In a geological regime, structural features are not always as dominant as shown in picture 11a. Consequently, the resulting binary images derived from photographs can contain a large quantity of error pixels. Pre-processing techniques such as filtering and subsequent processing based on specific characteristics of discontinuity traces are thus required to remove erroneous responses. Furthermore, when lines represent discontinuity traces, edge detectors produced a double response corresponding to the two sides of a line as shown in Fig. 11c to 11e. A method producing a systematic elimination of one of the responses could solve this problem.

In order to maintain high recognition and low error rates, individual threshold values were adjusted for each operator. Furthermore, after fine-tuning, an optimal threshold value was obtained for each image. The use of a different threshold value for each image is an inconvenience in the creation of an automatic mapping tool. If a more conservative threshold value was selected, this would eliminate this problem, but it would result in a larger number of erroneous responses requiring further filtering.

The grey level photographic images analysed in this work were taken in an underground environment with a flashlight normal to the rock mass exposure. This resulted in very weak contrasts complicating the recognition of discontinuity traces defined by edges. Based on the results of this study a new methodology was developed for taking pictures underground whereby the lighting source is oblique to the rock exposure. This can result in stronger contrasts in images and improved detection performance.

Most practising mining engineers recognize the importance of mapping. Unfortunately due to time and production constraints it is often given insufficient attention. This is becoming more and more critical in mining operations whereby access is often limited as a result of development and can be obscured by the application of supports such as shotcrete liners. A successful image analysis technique will contribute to alleviating these problems.

This note has presented work in progress towards developing a robust methodology suitable for characterising the structural regime of rock masses. None of the algorithms investigated in this study is independently reliable as a general tool

for extracting discontinuity trace maps from digital rock face images. An integrated approach distinguishing between edge and line structural features must be developed. The comparative study of different edge and line detectors clearly demonstrates the need for the development of further processing before seeking to quantify the rock engineering properties of interest.

Acknowledgements

The authors would like to acknowledge the financial support of the National Science & Engineering Research Council of Canada and Noranda Inc.

References

Allam, M. M. (1978): The estimation of fractures and slope stability of rock faces using analytical photogrammetry. Photogrammetria 34, 89–99.

Beer, G., Opriessnig, G., Golser, H., Fasching, A., Gaich, A. (1999): Geotechnical data acquisition, numerical simulation and visualization on site. In: Proc., Ninth International Congress on Rock Mechanics, Paris, France, 1333–1338.

Canny, J. (1986): A computational approach to edge detection. IEEE Trans. Pattern Anal. Mach. Intell. 8 (6), 679–698.

Cheung, L. C. C., Poniewerski, J. M., Ward, B., Leblanc, D., Thurley, M. J., Maconochie, A. P. (1996): SIROJOINT and SIROFRAG: New techniques for joint mapping and rock fragment size distribution measurement. In: Mohanty, B. H. (ed.), Rock fragmentation by blasting. 253–258.

Crosta, G. (1997): Evaluating rock mass geometry from photographic images. Rock Mech. Rock Engng. 30, 35–58.

Dony, R. D. (1988): Line detection on rock face images. M.A.Sc. Thesis, Univ. of Waterloo, Canada.

Feng, Q., Sjögren, P., Stephansson, O., Jing, L. (1999): Fracture mapping of exposed rock faces by Total Station method. In: Proc., Ninth International Congress on Rock Mechanics, Paris, France.

Gonzalez, R. C., Wintz, P. (1987): Digital image processing, 2 edn. Addison-Wesley, Boston.

Hadjigeorgiou, J., Lessard, J. F., Villaescusa, E., Germain, P. (1995): An appraisal of structural mapping techniques. In: Proc., 2nd Intl. Conf. Jointed and Faulted Rocks. Vienna, 191–197.

Hagan, T. O. (1980): A case of terrestrial photogrammetry in deep-mine rock structure studies. Int. J. Rock Mech. Min. Sci. 15, 191–198.

Harrison, J. P. (1993): Improved analysis of rock mass geometry using mathematical and phogrammetric methods. Ph.D. Thesis, University of London (Imperial College of Science, Technology and Medicine), U.K.

Johnson, R. P. (1990): Contrast based edge detection. Pattern Recogn. 23 (3–4), 311–318.

Lee, S. W., Kim, Y. J. (1995): Direct extraction of topographic features for gray scale character recognition. IEEE Trans. Pattern Anal. Mach. Intell. 17 (7), 724–729.

Maerz, N. H. (1990): Photoanalysis of rock fabric. Ph.D. Thesis, University of Waterloo, Canada.

Reid, T. R., Harrison, J. P. (2000): A semi-automated methodology for discontinuity trace detection in digital images of rock mass exposures. Int. J. Rock Mech. Min. Sci. 37, 1073–1089.

Rorke, A. J., Brummer, R. K. (1985): A stereographic mapping technique. In: Proc., SANGORM Symposium on Rockmass Characterisation, MINTEK, Randburg, 117–119.

Steger, C. (1998): An Unbiased Detector of Curvilinear Structures. IEEE Trans. Pattern Anal. Mach. Intell. 20 (2), 113–125.

Tsoutrelis, C. E., Exadactylos, G. E., Kapenis, A. P. (1990): Study of the rock mass discontinuity system using photoanalysis. In: Rossmanith, H. P. (ed.) Mechanics of Jointed and Faulted Rock. 103–112.

Wang, L., Pavlidis, T. (1993): Direct gray-scale extraction of features for character recognition. IEEE Trans. Pattern Anal. Mach. Intell. 15 (10), 1053–1066.

Authors' address: Prof. John Hadjigeorgiou, Université Laval, Department of Mining, Metallurgy and Materials Engineering, G1K 7P4 Quebec City, Quebec, Canada; e-mail: john.hadjigeorgiou@gmn.ulaval.ca